Transition modeling using data driven approaches

By K. Duraisamy† AND P.A. Durbin‡

An intermittency transport-based model for bypass transition is constructed by combining inverse modeling and machine learning. Data on the intermittency field for laminar to turbulent transition is extracted by adjoint-based optimization. This information is converted to modeling knowledge using machine learning techiques. The key significance of this approach is that it accounts for the operational role of intermittency within the context of RANS equations and thus does not suffer from inconsistencies that arise in *a priori* or *a posteriori* data extraction methods. The primary objective of this work is to demonstrate the potential for model-based, optimum data extraction and machine learning as valuable tools for turbulence and transition modeling.

1. Introduction

Accurate prediction of transition to turbulence in wall-bounded flows continues to be a pacing item in the computational modeling of fluid flows in many disciplines of science and engineering. A key difficulty in constructing models for transition (and turbulence) arises from the fact that intermediate dependent variables that appear in the model may take numerical values that are different from their physical values (as measured in an experiment or as computed from a Direct Numerical Simulation). Examples include the dissipation rate of kinetic energy ϵ or the intermittency function γ. Such quantities cannot be determined directly by data – either experimental or DNS - but must be inferred from the context of how these fields appear in the model. In this work, we propose a new way of extracting modeling information from data using inverse solutions and then using Machine Learning to convert information into modeling knowledge. This approach is applied to the case of modeling bypass transition using intermittency transport models. Specifically, we will use data from the T3-series of flat plate experiments (Roach & Brierley (1992)). This data set consists of two zero-pressure gradient test cases (T3A and T3B, with 3.5% and 6.5% turbulence intensity levels) and T3C1-C5 which have pressure gradients and turbulence intensities in the range of 3.4%-10%. The length-based Reynolds numbers for these test cases are in the range of $10^5 - 10^6$.

2. Bypass transition and intermittency transport models

When free-stream turbulence levels are about 1% or more, boundary layers typically proceed from laminar to fully turbulent states without the occurrence of linear instability of the base state: this mode of transition is referred to as bypass transition. Models of bypass transition for general CFD codes are a relatively recent development (Menter 2006) compared to natural transition. At a fundamental level, the bypass process occurs as turbulence diffuses into the laminar boundary layer and generates disturbances known as Klebanoff modes. These grow in amplitude, and transition to turbulence occurs

† Department of Aerospace Engineering, University of Michigan
‡ Department of Aerospace Engineering, Iowa State University

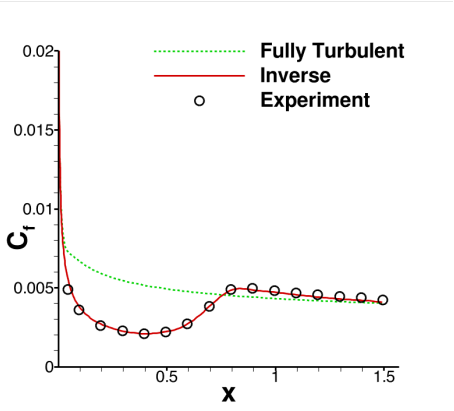

FIGURE 1. Result of inverse problem to match the experimental skin friction for the T3A test case (Roach & Brierley 1992). The initial condition assumes fully turbulent flow.

(Durbin & Wu 2007). Closure models, at RANS level, are very loosely based on this mechanism. One method is to use the concept of intermittency γ to blend the flow from the laminar to the turbulent regions. Intermittency is associated with the spottiness of turbulence and manifests itself as a non-Gaussian behavior in turbulent flows. An intermittency factor can be formally defined as a fraction of the time turbulence is active, and modeling strategies are roughly based on this definition.

Consider the $k-\omega$ closure (with values of the constants given by Wilcox (2006)) and the Reynolds-averaged Navier-Stokes equations. Transition can be introduced by multiplying the production term of the k equation by a function $\gamma(\boldsymbol{x})$. γ is zero in laminar flow, and ramps up to unity in fully turbulent flow. γ appears within the turbulence model only as a factor in the production term of the turbulent kinetic energy transport equation,

$$\frac{Dk}{Dt} = 2\nu_T|S|^2\boldsymbol{\gamma} - C_\mu k\omega + \partial_j\Big[\Big(\nu + \frac{\nu_T}{\sigma_k}\Big)\partial_j k\Big], \tag{2.1}$$

$$\frac{D\omega}{Dt} = 2C_{\omega 1}|S|^2 - C_{\omega 2}\omega^2 + \partial_j\Big[\Big(\nu + \frac{\nu_T}{\sigma_\omega}\Big)\partial_j \omega\Big]. \tag{2.2}$$

Here the eddy viscosity is given by $\nu_T = k/\omega$.

The model developed by Ge *et al.* (2014) is based on the idea that, in bypass transition under free-stream turbulence, non-zero γ diffuses into the boundary layer, allowing k to be produced, thereby creating eddy viscosity and further enhancing the diffusion of γ. In this way, transition occurs by penetration of free-stream turbulence into the boundary layer via molecular and turbulent diffusion. An intermittency transport equation is defined with a source term, P_γ, that contributes to producing intermittency inside the boundary layers. A sink term, E_γ, ensures that the boundary layer initially is laminar. The form of the model is

$$\frac{D\gamma}{Dt} = \partial_j\Big[\Big(\frac{\nu}{\sigma_l} + \frac{\nu_T}{\sigma_\gamma}\Big)\partial_j\gamma\Big] + P_\gamma - E_\gamma. \tag{2.3}$$

A detailed description of the model can be found in Ge *et al.* (2014).

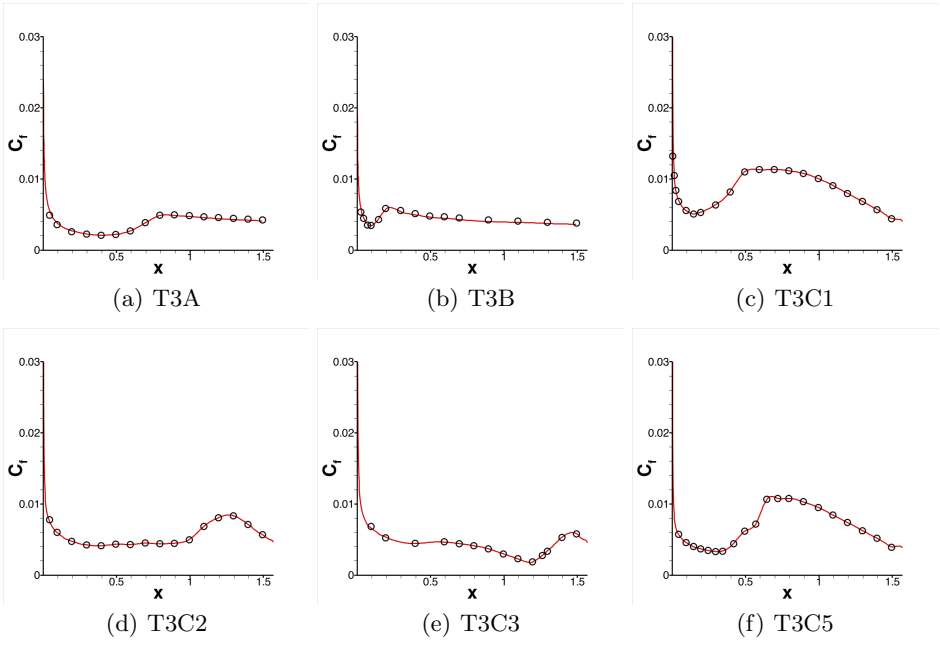

(a) T3A (b) T3B (c) T3C1

(d) T3C2 (e) T3C3 (f) T3C5

FIGURE 2. Inverse solution to match skin friction for T3-series of test cases. Symbols: data; lines: computation.

3. Inverse modeling approach

We begin with the question of determining the intermittency field that will be required within the context of Eq. (2.2) to match given data on transitional flows. For our problems of interest, skin friction measurements are available and thus we will choose an objective function of the form

$$\mathbf{G}(\gamma) = \int_w \left[\tau_w^{data}(s) - \tau_w^{model}(s)\right]^2 dS,$$

where the subscript w denotes the region of the wall surface that has available skin friction measurements. We will start with a fully turbulent assumption (i.e., $\gamma(\mathbf{x}) = 1$) and attempt to minimize $\mathrm{G}(\gamma)$ by considering every grid point value of γ as parameters in an optimization problem. A sample result of this inverse problem is shown in Figure 1. The output of the problem $\min_\gamma \mathrm{G}$ is thus a data field $\gamma(\mathbf{x})$ that is suited to the $k-\omega$ model. Note that intermittency is defined operationally, in terms of the model and the mechanism of ramping up the production term. It is not a physical variable that can be obtained from data, independently of its use. We consider this a paradigm for extracting data that are peculiar to a particular model, given other experimental or DNS data that the model predicts. This can be viewed as a method to introduce specific empiricism into models.

The optimization problem uses a gradient-based Quasi-Newton method employing the limited memory Broyden-Fletcher-Goldfarb-Shanno (LBFGS) algorithm (Dennis & More (1977)). Since the optimization problem is extremely high dimensional (as the number of parameters equals the number of mesh points), an adjoint solver is required to efficiently compute gradients. Consider the discretized governing equations (including boundary conditions) $\mathbf{R}_H = \mathbf{0}$ along with a discrete objective function $\mathrm{G}_H =$

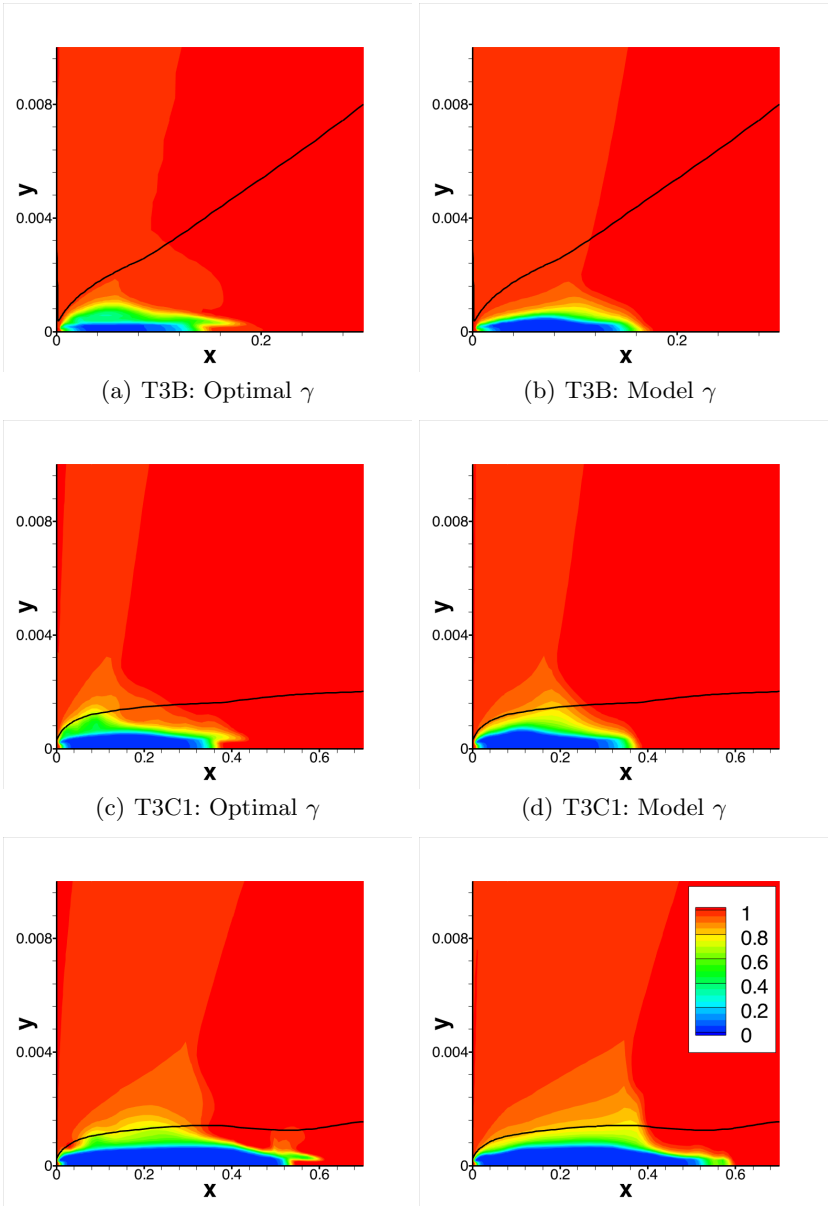

(a) T3B: Optimal γ (b) T3B: Model γ

(c) T3C1: Optimal γ (d) T3C1: Model γ

(e) T3C5: Optimal γ (f) T3C5: Model γ

FIGURE 3. Comparison of inferred intermittency field and the model of Ge *et al.* (2014) for selected cases, with the mean flow imposed from the inferred solution. The line is an iso-contour of 99% of the inlet free-stream velocity.

$\sum_{j=1}^{N_w} \left[\tau_{w,j}^{data} - \tau_{w,j}^{model}\right]^2 \Delta s_j$. The discrete adjoint equation (Giles & Pierce (2000)) for the vector of adjoint variables $\mathbf{\Psi}_H$ is given by

$$\left[\frac{\partial \mathbf{R}_H}{\partial \mathbf{Q}_H}\right]^T \mathbf{\Psi}_H = -\left[\frac{\partial \mathrm{G}_{.H}}{\partial \mathbf{Q}_H}\right]^T. \tag{3.1}$$

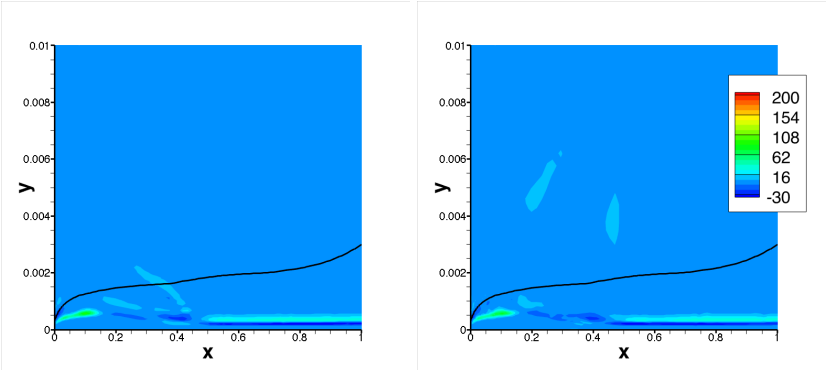

(a) Inferred source term (b) Predicted source term

FIGURE 4. Comparison of inferred source term and neural network prediction for T3C1.

In this work, the software suite ADOL-C (Griewank (1996)) has been used for automatic differentiation of the complete set of dependencies including the scalar transport variables. Given the adjoint solution, the gradient of the cost function with respect to the intermittency γ_i at every mesh point can computed as

$$\frac{d\mathbf{G}_H}{d\gamma_i} = \mathbf{\Psi}_H^T \frac{\partial \mathbf{R}_H}{\partial \gamma_i}$$

and used in the optimization loop.

Figure 2 shows the result of the inverse solution on the T3-series of test cases, confirming the effectiveness of the approach. The left column in Figure 3 shows the inferred intermittency field. The right column shows the intermittency field obtained using the transition model of Ge *et al.* (2014) with the mean flow imposed from the inferred solution. The most significant difference in the T3A and T3B cases is that the inferred field extends higher in the boundary layer near the inlet. This difference explains the the over prediction of C_f near the inlet in the original Ge *et al.* (2014) model and suggests that the sink term in Eq. (2.3) needs improvement.

The T3C1 case has a high level of free-stream turbulence and shows a prompt transition. Again the inferred field shows the low intermittency extending higher in the boundary layer, near the entrance, than the model. The T3C2 case has a lower free-stream intensity and lower Reynolds number than T3C1 and the C_f prediction in Ge *et al.* (2014) is fairly accurate; correspondingly, the inferred and modeled fields were confirmed to be fairly close. The cases presented here are representative of the other T3 cases: The inferred intermittency field shows the region of $\gamma < 1$ extending higher into the boundary layer near the inlet and the $\gamma = 1$ region is achieved farther inside the downstream boundary layer. The model postulates a sink term that is a function of $R_t \equiv \nu_T/\nu$ and $R_\nu \equiv d^2|\Omega|/2.188\nu$. It is not clear that the discrepancy between the model and inferred fields can be parametrized by these terms. In the next section, a new parametrization, based on machine learning is proposed to improve the model.

4. Machine Learning

The inverse approach presented in the previous sections results in an intermittency field $\gamma(\mathbf{x})$ that matches the experimental C_f data in each test case. This information can be translated into modeling knowledge by introducing a transport equation for the

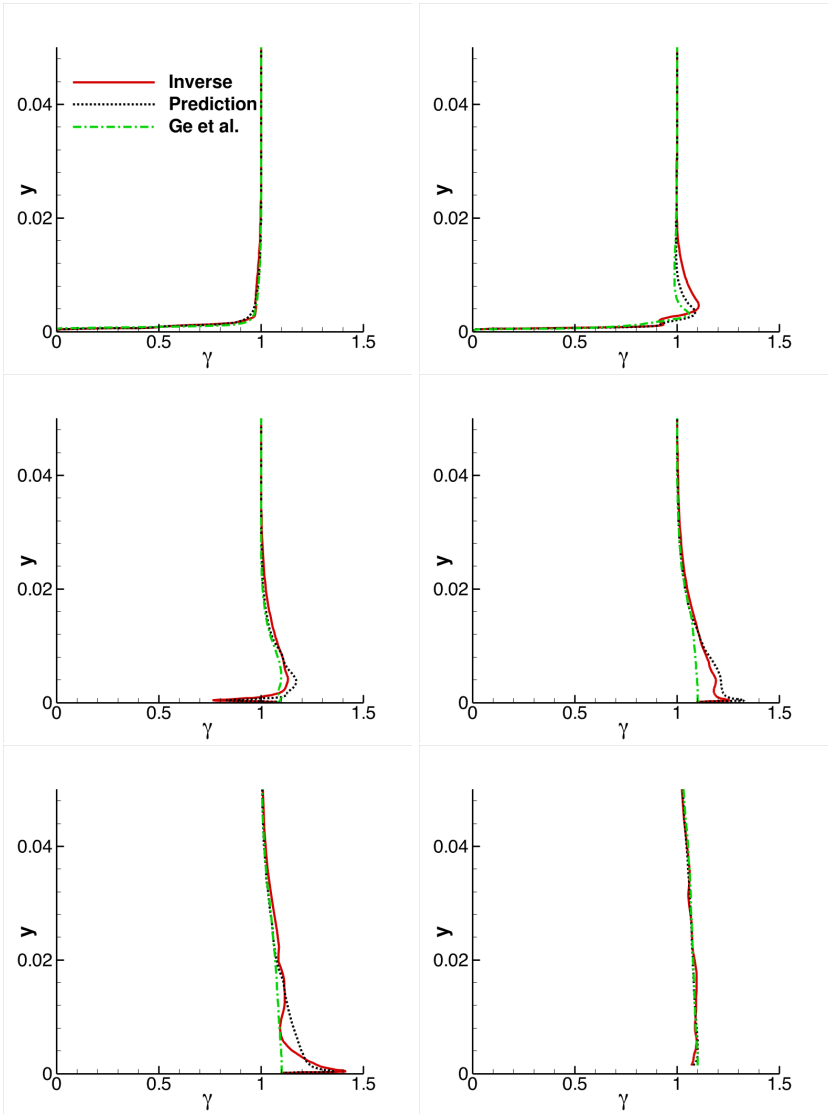

FIGURE 5. Intermittency field at selected streamwise stations for inferred, predicted and model for T3C1. Locations are x=0.1,0.2,0.4,0.6,1.0,1.5.

intermittency variable and supplementing the equation with terms that will be derived using machine learning techniques. This is a two-step process. For the first step, we write Eq. (2.3) as

$$\frac{D\gamma}{Dt} = \partial_j\Big[\Big(\frac{\nu}{\sigma_l} + \frac{\nu_T}{\sigma_\gamma}\Big)\partial_j\gamma\Big] + S_\gamma. \tag{4.1}$$

Thus, the production and destruction of intermittency will be computed by assuming that Eq. (4.1) is satisfied by the optimal intermittency field; in other words,

$$S_\gamma = \frac{D\gamma}{Dt} - \partial_j\Big[\Big(\frac{\nu}{\sigma_l} + \frac{\nu_T}{\sigma_\gamma}\Big)\partial_j\gamma\Big] \tag{4.2}$$

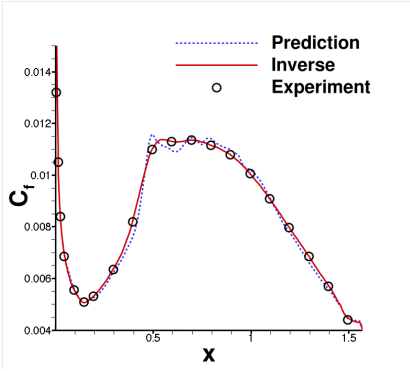

FIGURE 6. Skin friction prediction for T3C1.

In the second step, $S_\gamma(\mathbf{x})$ will be expressed, to some degree of approximation, as $S_\gamma(\boldsymbol{\xi})$, where $\boldsymbol{\xi} = \{\xi_1, \xi_2, ..., \xi_M\}$ is an M-dimensional parameter vector composed of local variables. Using supervised learning algorithms based on Artificial Neural Networks (ANN) as well as Gaussian Process Regression (GPR), we have chosen the combination

$$\boldsymbol{\xi} = \{k, \omega, \gamma, \frac{\partial u_i}{\partial x_j}, \nu\}$$

as a comprehensive parameter set. Figure 4 compares the predicted source term $S_\gamma(\boldsymbol{\xi})$ (using ANN) versus the actual source term $S_\gamma(\mathbf{x})$ via the inverse solution for the T3C1 transition case. The close agreement confirms the validity of the new parametrization. The inferred, predicted and model Ge *et al.* (2014) intermittency profiles are shown in Figure 5. The inadequacy of the model in predicting the high levels of intermittency required in the context of the $k-\omega$ closure is again confirmed. Note that, to attain the intensity of turbulence in the fully developed region, the intermittency variable needs to assume a value greater than unity. Figure 6 shows the ability of the machine learning method to reproduce the inferred skin friction results.

5. Summary

The results highlight the potential of inverse modeling and machine learning techniques to quantify and account for deficiencies in transition modeling. The optimal intermittency field is inferred from data and a transport equation is built to reproduce the inferred intermittency field. The proposed techniques are general enough to be applied in any modeling situation in which appropriate data is available. Continuing work is aimed at applying the methodology to a wider set of problems and operating the framework in a predictive mode.

Acknowledgments

This work was partially funded by the NASA Aeronautics Research Institute (NARI) under the Leading Edge Aeronautics Research for NASA (LEARN) program. The authors thank Juan Alonso and Brendan Tracey for their inputs in the project, and Shivaji Medida for help with neural network implementation.

REFERENCES

Ge, X., Arolla, S. & Durbin, P. 2014 A bypass transition model based on the intermittency function. *Flow Turbul. Combust.* **93**, 37–61.

Roach, P. E. & Brierley, D. H. 1992 The influence of a turbulent free-stream on zero pressure gradient transitional boundary layer development Part 1: Test cases T3A and T3B. In *Numerical Simulation of Unsteady Flows and Transition to Turbulence*, pp. 319–347, ERCOFTAC.

Savill, A.M. 1993 Some Recent Progress in Turbulence Modeling of By-pass Transition, *Near-Wall Turbulent Flows*, Elsevier.

Menter, F. R., Langtry, R., and Volker, S. 2006 Transition modelling for general purpose CFD codes. *Flow Turbul. Combust.* **77**, 277–303.

Durbin, P., and Wu, X. Transition beneath vortical disturbances. *Annu. Rev. Fluid Mech.* **39**, 107–128.

Giles, M., and Pierce, N. An introduction to the adjoint approach to design. *Flow, Turbul. and Combust.* **65**, 393-415.

Griewank, A., Juedes, D., and Utke, J. Algorithm 755: ADOL-C: A Package for the Automatic Differentiation of Algorithms Written in C/C++. *ACM Trans. Math. Soft.* **25** 131-167.

Dennis, J.E., and More, J. Quasi-Newton methods, motivation and theory. *SIAM Rev.* **19**, 46–89.

Wilcox, D. Turbulence modeling for CFD. Vol. 2, DCW Industries.